

## Ozone Production and Loss Rate Measurements in the Middle Stratosphere

K. W. Jucks, D. G. Johnson, K. V. Chance and W. A. Traub

*Harvard-Smithsonian Center for Astrophysics, Cambridge, Massachusetts, 02138*

R. J. Salawitch and R. A. Stachnik

*Jet Propulsion Laboratory, California Institute of Technology, Pasadena, California, 91109*

The first simultaneous measurements of  $\text{HO}_x$ ,  $\text{NO}_x$ , and  $\text{Cl}_x$  radicals in the middle stratosphere show that  $\text{NO}_x$  catalytic cycles dominate loss of ozone ( $\text{O}_3$ ) for altitudes between 24 and 38 km;  $\text{Cl}_x$  catalytic cycles are measured to be less effective than previously expected; and there is no "ozone deficit" in the photochemically dominated altitude range from 31 and 38 km, contrary to some previous theoretical studies.

### Introduction

Understanding the rate of removal of stratospheric ozone through catalytic cycles involving  $\text{HO}_x$  ( $\text{HO}_2$  and  $\text{OH}$ ),  $\text{NO}_x$  ( $\text{NO}_2$  and  $\text{NO}$ ), and halogen ( $\text{ClO}$  and  $\text{BrO}$ ) radicals is essential for assessing the response of ozone to anthropogenic and natural perturbations such as industrial release of chlorofluorocarbons (CFCs) and halons, emission of nitrogen oxides from subsonic and supersonic aircraft, rising levels of  $\text{N}_2\text{O}$  and  $\text{CH}_4$ , and enhanced levels of sulfate aerosols following volcanic eruptions.<sup>1-3</sup> In this paper we give the results of the first experiment to make simultaneous measurements of ozone-controlling radicals in the middle stratosphere, combine the results with an observationally constrained photochemical model, and show that production and loss of ozone are in photochemical equilibrium over much of this altitude region.

Recent calculations from models of the mid-latitude stratosphere give the following theoretical results: catalytic cycles involving  $\text{NO}_x$  radicals are expected to dominate ozone destruction from about 22 to 45 km, while  $\text{HO}_x$  cycles dominate both above and below;<sup>3-9</sup> and modeled photochemical loss of ozone exceeds modeled production by 10 to 50% in the upper stratosphere.<sup>4-8</sup> The latter finding has been coined the "ozone deficit" problem, because at these altitudes ozone is expected

to be in photochemical equilibrium (production equalling loss), since the photochemical lifetime of ozone is much shorter than transport replacement times.

The first finding has recently been tested below 21 km using in-situ aircraft measurements of  $\text{HO}_x$ ,  $\text{NO}_x$  and  $\text{Cl}_x$  radicals.<sup>10</sup> These measurements, made under conditions of high aerosol loading as a result of the eruption of Mt. Pinatubo, are in good agreement with models which include the heterogeneous hydrolysis reaction of  $\text{N}_2\text{O}_5$  on sulfate aerosols.<sup>3,4</sup>

The ozone deficit problem above 45 km has also been recently discussed,<sup>9</sup> using satellite measurements of several long lived species, with the result that estimated production and loss of ozone are in better agreement than had been found in previous analyses of other satellite data. However, this study lacks direct measurements of  $\text{HO}_x$  or  $\text{Cl}_x$  radicals.

In this paper, we use the the first simultaneous measurement of concentrations of  $\text{HO}_x$ ,  $\text{NO}_x$ ,  $\text{Cl}_x$ , and radical precursors throughout the middle stratosphere<sup>11</sup> to calculate the photochemical removal rate of ozone between 20 and 38 km. This analysis is the first to use direct and simultaneous measurements of radicals to determine the ordering of the loss cycles of ozone in the middle stratosphere, and to study the ozone deficit problem.

Diurnally averaged photochemical removal rates of  $\text{O}_3$  by each family of radicals are determined in two ways: from direct measurements of radical concentrations (radical method), and from radical concentrations calculated by a photochemical model constrained by measurements of radical precursors (precursor method). The radical method is used to derive, for the first time, empirical measures of the total loss rate of ozone as well as the relative removal rate by each family of radicals which regulate the abundance of ozone in the middle stratosphere (24-40 km). The precursor method provides a basis for comparing the empirical loss rates to theoretical rates constrained by appropriate environmental conditions, represented by the observed concentrations of long lived radical precursors. Empirical loss rates found using the radical method demonstrate that catalytic cycles involving  $\text{NO}_x$  radicals dominate photochemical removal of  $\text{O}_3$  in the middle

stratosphere, consistent with theoretical predictions using the precursor method. Our measurements demonstrate that production and loss rates of ozone (found using both methods) balance to within the uncertainty of measurement (10%) for altitudes between 31 and 38 km. This finding, which reconciles a long standing discrepancy in stratospheric chemistry, is due primarily to our observation of a lower abundance of ClO than calculated by models that allow for production of HCl only from the reaction of Cl and hydrocarbons.<sup>11</sup>

### Measurements and Model

Descriptions of the measurement technique and analysis methods<sup>12</sup> have been published previously; thus only a brief summary is given here. Data were acquired on a balloon flight launched from Ft. Sumner, New Mexico (34°N, 104°W) on 26-27 September, 1989. Concentrations of ClO were measured at mid-day between altitudes of 20 and 40 km with the Jet Propulsion Laboratory (JPL) Balloon Microwave Limb Sounder (BMLS), which senses microwave emission from the limb. Concentration profiles of OH, HO<sub>2</sub>, H<sub>2</sub>O<sub>2</sub>, HOCl, HCl, NO<sub>2</sub>, HNO<sub>3</sub>, N<sub>2</sub>O, H<sub>2</sub>O, O<sub>3</sub>, and temperature were measured throughout a diurnal cycle with the Smithsonian Astrophysical Observatory (SAO) far-infrared Fourier transform spectrometer (FIRS-2), which detects atmospheric thermal emission in a limb viewing geometry.

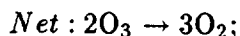
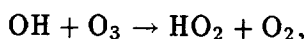
The constrained photochemical model used in our analysis balances, over a 24 hour period, the production and loss of 35 reactive gases for the temperature, pressure, and latitude at which the observations were obtained.<sup>13</sup> Standard reaction rates and absorption cross sections were used,<sup>14</sup> except that photolysis cross sections for H<sub>2</sub>O<sub>2</sub>, HNO<sub>2</sub>, and HNO<sub>4</sub> were extrapolated to longer wavelengths to accurately represent photolysis of these molecules at large solar zenith angles. A reaction probability of 0.1 was used for the heterogeneous hydrolysis of N<sub>2</sub>O<sub>5</sub>.<sup>14</sup> The heterogeneous hydrolysis of ClNO<sub>3</sub> and BrNO<sub>3</sub> were included,<sup>15</sup> but have a negligible effect on model results for the temperatures of these observations. The altitude profile for the surface area density of sulfate

aerosols was adopted from SAGE II extinction measurements for this time period.<sup>1</sup> Other inputs to the constrained photochemical model include the profiles of temperature, O<sub>3</sub>, and H<sub>2</sub>O measured by FIRS-2. Profiles of CH<sub>4</sub>, odd nitrogen (NO<sub>y</sub> = NO + NO<sub>2</sub> + NO<sub>3</sub> + 2xN<sub>2</sub>O<sub>5</sub> + HNO<sub>2</sub> + HNO<sub>3</sub> + HNO<sub>4</sub> + ClNO<sub>3</sub> + BrNO<sub>3</sub>), inorganic chlorine (Cl<sub>y</sub> = HCl + ClNO<sub>3</sub> + ClO + HOCl + Cl + OClO + 2xCl<sub>2</sub>O<sub>2</sub> + ClOO), and inorganic bromine (Br<sub>y</sub> = HBr + BrONO<sub>2</sub> + BrO + HOBr + BrCl) have been inferred from the FIRS-2 measurement of N<sub>2</sub>O using relations derived from previous satellite<sup>16</sup> and in situ observations.<sup>17</sup> The maximum Br<sub>y</sub> at high altitude is assumed to be 21 ppt.

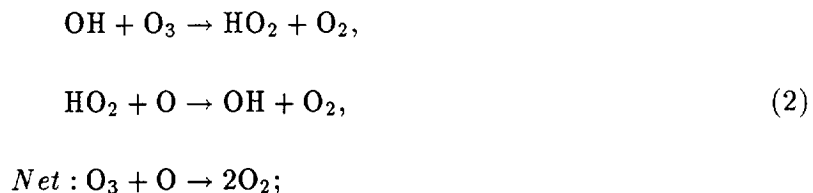
### O<sub>3</sub> Photochemical Loss and Production Rates

Ozone and atomic oxygen (O), together defined as odd oxygen (O<sub>x</sub>), are in rapid photochemical steady state via the reactions O<sub>3</sub>+hν → O+O<sub>2</sub> and O+O<sub>2</sub>+M → O<sub>3</sub>+M. Throughout the stratospheric altitude range discussed in this paper, O<sub>3</sub> represents more than 99% of total odd oxygen, thus a change in the abundance of odd oxygen is considered as equivalent to a change in the abundance of O<sub>3</sub>. Oxides of hydrogen, nitrogen, chlorine, and bromine regulate the abundance of O<sub>x</sub> in the middle stratosphere through a variety of reactions that catalyze the self reaction of O<sub>3</sub> or the reaction of O<sub>3</sub> and atomic oxygen. Since each reaction sequence listed below accounts for the loss of two molecules of O<sub>x</sub>, the net loss rates are determined by doubling the diurnally averaged rate of the limiting step (indicated by the number label) of each cycle.

The role of HO<sub>x</sub> radicals in regulating the abundance of odd oxygen was first noted by Bates and Nicolet.<sup>18</sup> The important cycles are:

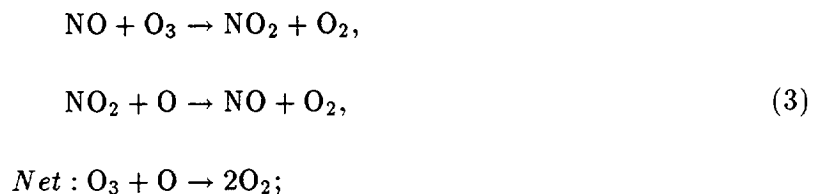


and

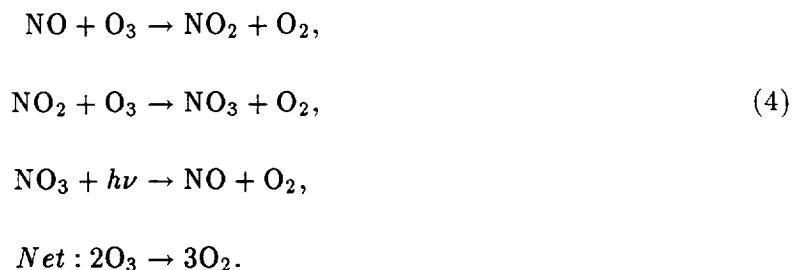


with other cycles accounting for less than 5% of ozone loss by  $\text{HO}_x$  species between 35 and 40 km, and less than 1% below 35 km.

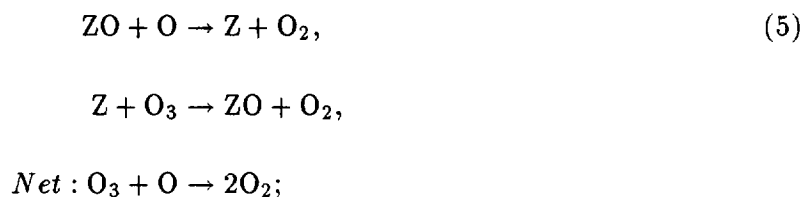
Crutzen<sup>19</sup> and Johnston<sup>20</sup> established the importance of removal of odd oxygen by cycles involving  $\text{NO}_x$  :



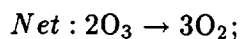
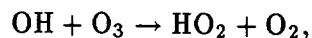
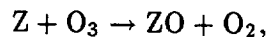
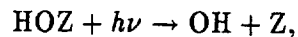
and



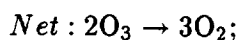
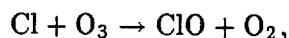
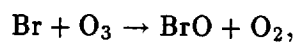
Molina and Rowland<sup>21</sup> and Wofsy *et al.*<sup>22</sup> drew attention to removal of odd oxygen by chlorine and bromine radicals, respectively. Loss occurs primarily through the cycles:



and



where  $\text{Z} = \text{Cl}$  or  $\text{Br}$ , as well as through the cycle



which is a major loss cycle for  $\text{O}_3$  in the Antarctic spring.

Loss of odd oxygen proceeds also by the reaction:<sup>23</sup>



which is a minor sink in the middle stratosphere. Odd oxygen is produced by photolysis of  $\text{O}_2$  at wavelengths shorter than 200 nm, with a small contribution from the reaction of  $\text{CH}_3\text{O}_2$  and  $\text{NO}$ .<sup>10</sup>

The precursor method uses a photochemical model, constrained by our measurements of  $\text{O}_3$ ,  $\text{H}_2\text{O}$ ,  $\text{N}_2\text{O}$ , and temperature, to predict the abundances of  $\text{O}$ ,  $\text{HO}_2$ ,  $\text{OH}$ ,  $\text{NO}_2$ ,  $\text{ClO}$ , and  $\text{BrO}$  over a 24 hour period. These abundances are used to calculate the rates of reactions 1–8. The loss rates of  $\text{O}_3$  are integrated over 24 hours, using the DeMore *et al.* reaction rate constants,<sup>14</sup> and summed to evaluate the the rates of the  $\text{HO}_x$  (1+2),  $\text{NO}_x$  (3+4), halogen (5+6+7), and  $\text{O}+\text{O}_3$  (8) loss cycles.

The radical method uses direct measurements of  $\text{HO}_2$ ,  $\text{OH}$ ,  $\text{NO}_2$ , and  $\text{ClO}$  to calculate the rates of reactions 1–8. The measurements are interpolated onto a finer time grid by normalizing the abundances calculated by the constrained photochemical model to best fit the data. This process is shown in Figure 1 for a representative altitude of 32 km. We note that the model is in excellent agreement with the data even before scaling. We include 1 sigma uncertainties in the observations, plus any residuals between the observed and normalized concentrations.

Figure 2 compares the removal rate of odd oxygen from the radical and precursor methods, partitioned into each radical family. This figure illustrates that the general behavior of the removal rates of odd oxygen inferred from the observed concentration of radicals is in broad agreement with theory for the  $\text{HO}_x$  and  $\text{NO}_x$  families of radicals. Theoretical values for the loss rate due to halogen cycles are calculated using two models: a conventional model which allows for production of  $\text{HCl}$  only by reactions of  $\text{Cl}$  with hydrocarbons (a typical assumption of current multi-dimensional models of atmospheric photochemistry and transport<sup>3,24,25</sup>); and a second model which includes additional production of  $\text{HCl}$  from a 10% branch of the reaction of  $\text{ClO}$  with  $\text{OH}$ . DeMore et al.<sup>14</sup> suggests a lower limit of 0%, and an upper limit of 14%, for production of  $\text{HCl}$  from the  $\text{ClO}+\text{OH}$  reaction. Laboratory measurements of  $\text{HCl}$  from this reaction, which would involve breaking and reformation of multiple chemical bonds, give ambiguous results. Our observations of  $\text{ClO}$  (see figure 1), supported by our simultaneous measurements of  $\text{OH}$ ,  $\text{HO}_2$ ,  $\text{HOCl}$ , and  $\text{HCl}$ ,<sup>11</sup> give best agreement with the the second model. Above 32 km, the lower abundance of  $\text{ClO}$  calculated by the second model gives removal rates of ozone by halogens which are reduced by as much as 40% compared to the conventional model. While this reaction is not the only possible pathway for additional production of  $\text{HCl}$  which might be consistent with the simultaneous measurement of  $\text{ClO}$ ,  $\text{HOCl}$  and  $\text{HCl}$ , it is the only pathway within suggested uncertainties of current kinetics measurements.<sup>14</sup> Corroborating evidence for the existence of such an additional pathway for production of  $\text{HCl}$  is provided by ATMOS measurements of  $\text{HCl}$  and  $\text{ClNO}_3$ <sup>6</sup>, and

UARS measurements of HCl, ClO, and ClNO<sub>3</sub>.<sup>26</sup>

The fractional contribution of each radical family to loss of odd oxygen is shown in Figure 3. Cycles involving NO<sub>x</sub> radicals dominate the loss of ozone between altitudes of 24 to 38 km, contributing a maximum of 66% to the total loss rate at 32 km. In contrast to observations obtained during SPADE,<sup>10</sup> our measurements also suggest that loss of odd oxygen due to NO<sub>x</sub> cycles is comparable to loss due to halogen cycles near 20 km. The SPADE measurements showed loss of odd oxygen due to NO<sub>x</sub> cycles to be a factor of 2-4 slower than loss due to halogen and HO<sub>x</sub> cycles. However, the large uncertainties of our measurements at these altitudes make it difficult to determine precisely the ordering of the loss cycles. The balloon-borne observations were obtained in 1989, when concentrations of Cl<sub>y</sub> were approximately 14% lower than contemporary levels<sup>27</sup> and sulfate aerosol loading was about a factor of 5 less than values encountered during SPADE, which were elevated due to the eruption of Mt. Pinatubo in the summer of 1991. Both factors contribute to a larger relative contribution by NO<sub>x</sub> cycles to odd oxygen removal in the lower stratosphere during 1989.

Figure 4 illustrates diurnally averaged total loss rates for odd oxygen inferred from both the radical and precursor methods, as well as production rates from photolysis of O<sub>2</sub> calculated using a radiative transfer model that includes Rayleigh and aerosol scattering.<sup>6,28</sup> Three conclusions can be drawn from this figure. First, odd oxygen loss rates inferred from the observed concentrations of radicals (radical method) agree with theoretical loss rates (precursor method) to within the measurement uncertainty at all altitudes. Second, between 31 and 38 km, where the photochemical lifetime of ozone is short, we find that production and loss rates of odd oxygen calculated using both methods balance to within the uncertainty of the measurements of the radicals (approximately 10%), in contrast to previous studies (which lacked simultaneous measurements of HO<sub>2</sub>, NO<sub>2</sub>, and ClO) that reported loss rates up to 50% greater than production rates.<sup>4-8</sup> Third, rates of production below 31 km exceed the loss rates calculated using both methods by 30 to 40%, indicating that



this region is a net photochemical source region for  $O_3$ . This imbalance is consistent with results of 2-dimensional photochemical-transport models that show production and subsequent transport of  $O_3$  to higher latitudes from this region.<sup>8,29</sup>

Our finding that production and measured loss of odd oxygen balance for altitudes between 31 and 38 km differs from the results of previous studies for two reasons: (i) we observe lower concentrations of ClO at these altitudes than are predicted by models which assume that production of HCl occurs only by reaction of Cl with hydrocarbons,<sup>11</sup> as illustrated in Figure 1; and (ii) we use a formulation for photolysis of  $O_2$  that results in deeper penetration of ultraviolet radiation,<sup>6</sup> and better agreement with measured transmittances, than is found using the formulation recommended by WMO.<sup>30</sup> Including the additional source of HCl lowers the total modeled loss rate of odd oxygen by about 17% near 38 km resulting in close agreement between production and loss of ozone found using the precursor method. Our findings are consistent with the study of Minschwaner *et al.*,<sup>6</sup> who postulated, based on constraints imposed by Atmospheric Trace Molecule Spectroscopy Experiment (ATMOS) measurements of  $O_3$ , NO,  $NO_2$ ,  $N_2O_5$ ,  $HNO_3$ ,  $ClNO_3$ , HCl,  $H_2O$ , and  $CH_4$ , that production and loss of odd oxygen would balance near 40 km if a minor branch of the reaction of ClO with OH results in production of HCl. Similar conclusions were reached by Chandra *et al.*,<sup>31</sup> who found that submillimeter heterodyne measurements of ClO and HCl<sup>32</sup> and the observed abundance and seasonal variation of  $O_3$  near 40 km were better simulated by allowing for the additional pathway for production of HCl. A more recent theoretical study<sup>9</sup> on the balance of production and loss of odd oxygen based on constraints provided by HALOE measurements of HCl,  $H_2O$ , and  $O_3$  found a balance between production and loss between 35 and 40 km and excess production above 45 km.

## Discussion

Most current models which are used to assess the impact of anthropogenic emission of halogens on ozone overestimate the abundance of ClO in the upper stratosphere by neglecting the possibility of an additional pathway for production of HCl.<sup>24</sup> Our observations demonstrate that these models overestimate the relative contribution of halogen cycles to the removal rate of odd oxygen at altitudes near 40 km. The predicted decrease in ozone near 40 km resulting from the build up of halogens during the past several decades is mitigated by 50% if an additional pathway for production of HCl is included in models, resulting in closer agreement between observed and predicted trends in O<sub>3</sub> at these altitudes.<sup>31</sup> Above 45 km, HO<sub>x</sub> catalyzed cycles dominate ozone loss, with the importance of halogen cycles decreasing with higher altitude into the mesosphere. Inclusion of an additional source of HCl may not be sufficient to solve the imbalance between modeled production and loss at altitudes where reaction 2 dominates loss of odd oxygen.<sup>5</sup> The recent study of Crutzen et al.<sup>9</sup> based on HALOE measurements of HCl, H<sub>2</sub>O and O<sub>3</sub> suggests excess production of ozone above 45 km. However, Crutzen et al. relied on theoretical profiles for OH and HO<sub>2</sub>. New observations of HO<sub>x</sub> radicals will be necessary to advance our understanding of the budget of O<sub>3</sub> at altitudes higher than 38 km.

Since the loss rates found using the radical method depend on measured radical and O<sub>3</sub> concentrations and not modeled values for radical concentrations, the uncertainties in the calculated loss rates are dependent primarily on the measurement uncertainties and rate constant uncertainties in the rate limiting steps. At the altitudes where we measure a balance between production and loss of odd oxygen, 32 and 38 km, the dominant odd oxygen loss cycles involve reactions 2, 3, 5 and 8, with reaction 3 contributing more than 60% to the odd oxygen loss. Reaction 5 is dominated by the ClO reaction, which is more than 2 orders of magnitude more effective than the BrO reaction at destroying odd oxygen above 30 km. As a result, uncertainties caused by using modeled BrO at these

altitudes are very small with respect to other errors being considered. Using the average measured temperature of 240 K for these altitudes, the uncertainties in the rate constants for reactions 2,3,5, and 8 are 30%, 21%, 27% and 40%, respectively. By weighting these uncertainties by the relative contributions from each of these cycles, we calculate a net uncertainty in the calculated total loss rate of 23%. This value is on the order of the estimated uncertainty (20%) in the production of  $\text{O}_3^6$  and is larger than the uncertainties (10%) in the loss rates calculated from the measurements of the radicals.

The accuracy of this set of radical measurements in the middle stratosphere, combined with the consistency between loss rates found using the radical and precursor methods, demonstrates that our first order understanding of processes that regulate the partitioning of radicals is correct, and that models, provided they allow for production of HCl either by the reaction of ClO and OH, or some other currently unknown process which results in similar chlorine partitioning, should provide a realistic description of the relative rate of removal of odd oxygen in the lower and middle stratosphere by each of the major catalytic cycles.<sup>3</sup>

#### References

1. "Scientific Assessment of Ozone Depletion: 1991, Global Ozone Research and Monitoring Project", *WMO-Report no. 25* (1991).
2. R. S. Stolarski and H. L. Wesoky, Eds., *NASA Ref. Publ. No. 1313* (1993).
3. J. M. Rodriguez *et al.*, *Geophys. Res. Lett.*, **21**, 209 (1994).
4. M. B. McElroy, R. J. Salawitch, K. Minschwaner, *Planet. Space Sci.*, **40**, 373 (1992).
5. P. J. Crutzen and U. Schmailzl, *Planet. Space Sci.*, **31**, 1009 (1983); L. Froidevaux, M. Allen, Y. L. Yung, *J. Geophys. Res.*, **90**, 12999, (1985); Eluszkiewicz, J. and M. Allen, *J. Geophys. Res.*, **98**, 1069 (1993).
6. K. Minschwaner, R. J. Salawitch, M. B. McElroy, *J. Geophys. Res.*, **98**, 10543 (1993).

7. M. B. McElroy and R. J. Salawitch, *Science*, **243**, 763 (1989).
8. Jackman, C. H., R. S. Stolarski, J. A. Kaye *J. Geophys. Res.*, **91**, 1103 (1986).
9. P. J. Crutzen, J.-U. Grooss, C. Bruhl, R. Muller, J. M. Russell III, *Science*, **268**, 705 (1995).
10. P. O. Wennberg, *et al.*, *Science*, **266**, 398 (1994).
11. K. V. Chance *et al.*, *J. Geophys. Res.*, submitted for publication. The simultaneous measurements of profiles for HCl, ClO, and HOCl in this study are statistically in better agreement with a model which include a 10% branching of the ClO+OH reaction to form HCl+O<sub>2</sub> than with a model which uses only the standard pathways for HCl formation.
12. W. A. Traub, K. V. Chance, D. G. Johnson, K. W. Jucks, *S.P.I.E.*, **1491**, 298 (1991); D. G. Johnson, K. W. Jucks, W. A. Traub, K. V. Chance, *J. Geophys. Res.*, **100**, 3091 (1995); J. W. Waters, J. C. Hardy, R. F. Jarnot, H. M. Pickett, P. Zimmermann, *J. Quant. Spectros. Radiat. Transfer*, **32**, 407 (1984).
13. R. J. Salawitch *et al.*, *Geophys. Res. Lett.*, **21**, 2547 (1994).
14. W. B. DeMore *et al.*, "Chemical Kinetics and Photochemical Data for Use in Stratospheric Modeling, Evaluation Number 11", (JPL Publication 94-26), Jet Propulsion Laboratory (1994).
15. D. R. Hanson and A. R. Ravishankara, *J. Phys. Chem.*, **98**, 5728 (1994); D. R. Hanson and E. R. Lovejoy, *Science*, **267**, 1326 (1995); D. R. Hanson and A. R. Ravishankara, *Geophys. Res. Lett.*, **22**, 385 (1995).
16. M. R. Gunson *et al.*, *J. Geophys. Res.*, **95**, 13867 (1990).
17. D. W. Fahey *et al.*, *Nature*, **344**, 321 (1990); J. W. Woodbridge *et al.*, *J. Geophys. Res.*, **100**, 3057 (1995); S. M. Schauffler *et al.*, *Geophys. Res. Lett.*, **20**, 2567 (1993).
18. D. R. Bates and M. Nicolet, *J. Geophys. Res.*, **55**, 301 (1950).
19. P. J. Crutzen, *Q. J. R. Meteorol. Soc.*, **96**, 320 (1970).
20. H. Johnston, *Science*, **173**, 517 (1971).
21. M. J. Molina and F. S. Rowland, *Nature*, **249**, 810 (1974).

22. S. C. Wofsy, M. B. McElroy, Y. L. Yung, *Geophys. Res. Lett.*, **2**, 215 (1975).
23. S. Chapman, *Phil. Mag.*, **10**, 369 (1930).
24. M. J. Prather and E. E. Remsberg, Eds., *NASA Ref. Publ. No. 1292, Vol II* (1993).
25. D. K. Weisenstein, M. K. W. Ko, J. M. Rodriguez, N. D. Sze, *J. Geophys. Res.*, **98**, 23133 (1993).
26. R. S. Eckman *et al.*, *J. Geophys. Res.*, **100**, 13951 (1995).
27. J. W. Elkins *et al.*, *Nature*, **364**, 780 (1993).
28. M. J. Prather, *J. Geophys. Res.*, **86**, 5325 (1981).
29. L. M. Perliski, S. Solomon, J. London, *Planet. Space Sci.*, **37**, 1527 (1989).
30. "Atmospheric ozone 1985: Assessment of our Understanding of the Processes Controlling its Present Distribution and Change, Global Ozone Research and Monitoring Project", *WMO-Report no. 16* (1986).
31. S. Chandra, C. H. Jackman, A. R. Jackman, E. L. Fleming, D. B. Considine, *Geophys. Res. Lett.*, **20**, 351 (1993).
32. R. A. Stachnik, J. C. Hardy, J. A. Tarsala, J. W. Waters, *Geophys. Res. Lett.*, **19**, 1931 (1992).
33. We are grateful to the Jet Propulsion Laboratory Atmospheric Ballooning group for gondola support and to the National Scientific Balloon Facility for launch services. The work at SAO was supported by NASA grant NSG-5175. Part of this research was performed at the Jet Propulsion Laboratory, California Institute of Technology, under contract with NASA.

## Figure Captions

Fig. 1. Individual concentration measurements (solid circles) are shown along with the modeled diurnal concentrations (solid curves) and the corresponding scaled concentrations (dotted curves) for  $\text{HO}_2$ ,  $\text{NO}_2$  and  $\text{ClO}$  at 32 km. The 1 sigma uncertainties are dominated by random measurement errors but include estimated systematic errors. The modeled  $\text{ClO}$  is also shown for the case of no production of  $\text{HCl}$  from the  $\text{ClO} + \text{OH}$  reaction (dashed curve). For this altitude, the average integration time for each measurement is 22, 42, and 50 minutes for  $\text{HO}_2$ ,  $\text{NO}_2$ , and  $\text{ClO}$ , respectively; each integration comprises several shorter observations spread over average corresponding intervals of 2, 5.5, and 7 hours.

Fig. 2.  $\text{HO}_x$  (solid triangles),  $\text{NO}_x$  (solid squares), and halogen (solid circles) catalyzed loss rates of  $\text{O}_3$  inferred from radical method and calculated using the precursor method (curves). Two halogen catalyzed precursor method loss calculations are illustrated: one assuming  $\text{HCl}$  production only from  $\text{Cl}$  reacting with hydrocarbons and one with additional production of  $\text{HCl}$  from a 10% branch of the  $\text{OH} + \text{ClO}$  reaction (see text). The  $\text{O} + \text{O}_3$  reaction curve can be considered to represent both the radical and precursor methods since  $\text{O}$  is inferred directly from measurements of  $\text{O}_3$ , which is the precursor for  $\text{O}$ . The symbols are offset in altitude for clarity.

Fig. 3. The fractional total loss of odd oxygen from the  $\text{HO}_x$ ,  $\text{NO}_x$ , and halogen catalytic cycles is shown as a function of altitude, as inferred from the radical method using measurements of  $\text{HO}_2$ ,  $\text{NO}_2$ ,  $\text{ClO}$  and  $\text{O}_3$  (symbols), and from the precursor method (curves).

Fig. 4. Loss rates of ozone calculated with the radical method (see text) from direct measurements of  $\text{HO}_2$ ,  $\text{NO}_2$ ,  $\text{ClO}$ , and  $\text{O}_3$  (solid circles), loss rates calculated using the precursor method (dotted curve), and production rates of  $\text{O}_3$  (solid curve) calculated primarily from photodissociation of  $\text{O}_2$  (see text) and constrained by measurements of  $\text{O}_3$  and temperature.

